THE NEW NEUTRON NOISE SOLVER OF THE MONTE CARLO CODE TRIPOLI-4®

Amélie Rouchon, Walid Jarrah and Andrea Zoia
DEN-Service d'études des réacteurs et de mathématiques appliquées (SERMA),
CEA, Université Paris-Saclay, F-91191, Gif-sur-Yvette, France.

amelie.rouchon@cea.fr, walid.jarrah@cea.fr, andrea.zoia@cea.fr

ABSTRACT

Neutron noise appears as fluctuations of the neutron field induced by vibrations of fuel elements, control rods or any other mechanical structures in the core, as well as from global or local fluctuations in the flow, density or void fraction of the coolant. Neutron noise equations are obtained by assuming small perturbations of macroscopic cross-sections around a steady-state neutron field and by subsequently taking the Fourier transform in the frequency domain. Recently, a new Monte Carlo algorithm was proposed in order to solve the transport equation in neutron noise theory with complex-valued weights and a modified collision operator. This paper presents the new neutron noise solver based on these methods and implemented in the reference Monte Carlo code TRIPOLI-4® developed at CEA. We illustrate the capabilities of the solver by considering the noise analysis of a UOX PWR assembly.

KEYWORDS: Neutron noise, Monte Carlo, TRIPOLI-4® , Frequency domain, Complex statistical weights.

1. INTRODUCTION

Neutron noise analysis addresses the description of time-dependent flux fluctuations induced by small global or local perturbations of the macroscopic cross-sections, which may occur in nuclear reactors due to stochastic density fluctuations of the coolant, to vibrations of fuel elements, control rods, or any other structures in the core [1]. Neutron noise techniques are adopted in the nuclear industry for non-invasive general monitoring, control and detection of anomalies in nuclear power plants [2]. They are also applied to the measurement of the properties of the coolant, such as speed and void fraction.

The general noise equations are obtained by assuming small perturbations around a steady-state neutron flux and by subsequently taking the Fourier transform in the frequency domain. The outcome of the Fourier transform analysis is a fixed-source equation with complex operators for the perturbed neutron field, which can then be solved so as to predict noise measurements at detector locations.

Until recently, neutron noise equations have been only solved by analytical techniques [3] and by resorting to diffusion theory [4,5]. It is therefore necessary to validate these approaches via Monte Carlo simulation. In 2013, a Monte Carlo algorithm was first proposed in order to solve

the transport equation in neutron noise theory [6,7]. Such algorithm is a cross-over between fixed-source and power iteration methods and adopts a weight cancellation technique. This method yields satisfactory results but has some shortcomings, such as the need of introducing a "binning procedure" for the weight cancellation: each fissile region must be divided into a large number of small regions where positive and negative weights are summed up and cancelled. In 2016, a second Monte Carlo algorithm was proposed [8]: contrary to [6], this method uses the conventional algorithm for fixed-source problems for all frequencies, does not need any weight cancellation technique, and is based on a modified collision kernel with a real total cross-section.

In this work, we present the new neutron noise solver based on this second Monte Carlo algorithm and implemented in the reference Monte Carlo code TRIPOLI-4® developed at CEA [9]. This paper is organized as follows. In Sec. 2, the general neutron noise theory will be briefly introduced and the Monte Carlo algorithm implemented in TRIPOLI-4® will be presented. In Sec. 3, we will verify our Monte Carlo solver by comparison with some analytical solutions. In Sec. 4, we will illustrate the capabilities of the proposed Monte Carlo solver by performing the analysis of neutron noise for a standard UOX PWR assembly. Conclusions will be drawn in Sec. 5.

2. DESCRIPTION OF THE NEW TRIPOLI-4® NEUTRON NOISE SOLVER

2.1. Neutron noise theory

The general noise equations are obtained by assuming small perturbations $\Psi(\mathbf{r},\mathbf{\Omega},E,t) = \Psi_0(\mathbf{r},\mathbf{\Omega},E) + \delta\Psi(\mathbf{r},\mathbf{\Omega},E,t)$ (which allows for a linear theory) around a steady-state neutron flux Ψ_0 and by subsequently taking the Fourier transform in the frequency domain. The analysis is performed based on the neutron kinetic equations, including the coupling with neutron precursors. The outcome of the Fourier transform analysis is a fixed-source equation with complex operators for the perturbed neutron field $\delta\Psi$, which can then be solved so as to predict noise measurements at detector locations. For each frequency, the perturbed neutron flux is a complex function having an amplitude and a phase. Imposing a periodic perturbation of the kinetic operator, the noise equation reads [1]:

$$\begin{aligned}\left(\mathbf{\Omega}\cdot\nabla + \Sigma_0(\mathbf{r},E) + i\frac{\omega}{v}\right)\delta\Psi(\mathbf{r},\mathbf{\Omega},E,\omega) = &\iint \Sigma_{0,s}(\mathbf{r},\mathbf{\Omega}'\cdot\mathbf{\Omega},E'\to E)\delta\Psi(\mathbf{r},\mathbf{\Omega}',E',\omega)dE'd\mathbf{\Omega}' \\ &+ \frac{1}{k}\frac{\chi_p(E)}{4\pi}\iint \nu_p(E')\Sigma_{0,f}(\mathbf{r},E')\delta\Psi(\mathbf{r},\mathbf{\Omega}',E',\omega)dE'd\mathbf{\Omega}' \\ &+ \frac{1}{k}\sum_j \frac{\chi_d^j(E)}{4\pi}\iint \nu_{d,\omega}^j(E')\Sigma_{0,f}(\mathbf{r},E')\delta\Psi(\mathbf{r},\mathbf{\Omega}',E',\omega)dE'd\mathbf{\Omega}' + S(\mathbf{r},\mathbf{\Omega},E,\omega),\end{aligned} \tag{1}$$

where i is the imaginary unit, $\omega = 2\pi f$ the angular frequency, and

$$\nu_{d,\omega}^j(E) = \left(\frac{\lambda_j^2 - i\lambda_j\omega}{\lambda_j^2+\omega^2}\right)\nu_d^j(E) \tag{2}$$

for the precursor family j; all other notations are standard. Thus, because of the delayed neutrons, the production operator depends on the frequency ω. Equation (1) can be conceptually split into a system of two equations for the real and imaginary part of $\delta\Psi$. The two equations are formally coupled by two terms: $i\omega/v$ and the modified delayed production operator including the complex

multiplicity $\nu^j_{d,\omega}(E)$. The noise source S is defined by:

$$S(\mathbf{r},\mathbf{\Omega},E,\omega) = -\delta\Sigma(\mathbf{r},E,\omega)\Psi_0(\mathbf{r},\mathbf{\Omega},E) + \iint \delta\Sigma_s(\mathbf{r},\mathbf{\Omega}'\cdot\mathbf{\Omega},E'\rightarrow E,\omega)\Psi_0(\mathbf{r},\mathbf{\Omega}',E')dE'd\mathbf{\Omega}'$$
$$+ \frac{1}{k}\frac{\chi_p(E)}{4\pi}\iint \nu_p(E')\delta\Sigma_f(\mathbf{r},E',\omega)\Psi_0(\mathbf{r},\mathbf{\Omega}',E')dE'd\mathbf{\Omega}'$$
$$+ \frac{1}{k}\sum_j \frac{\chi^j_d(E)}{4\pi}\iint \nu^j_{d,\omega}(E')\delta\Sigma_f(\mathbf{r},E',\omega)\Psi_0(\mathbf{r},\mathbf{\Omega}',E')dE'd\mathbf{\Omega}', \quad (3)$$

where $\delta\Sigma_x(\mathbf{r},E,\omega)$ is the Fourier transform of the perturbed term of the macroscopic cross-section $\Sigma_x(\mathbf{r},E,t) = \Sigma_{0,x}(\mathbf{r},E) + \delta\Sigma_x(\mathbf{r},E,t)$ with $\Sigma_{0,x}$ the static macroscopic cross-section.

2.2. The Monte Carlo algorithm implemented in TRIPOLI-4®

We briefly sketch the Monte Carlo algorithm that we have chosen to implement in the reference Monte Carlo code TRIPOLI-4®; a thorough description is given in [8]. Similarly as in [6], our method is based on the simulation of particles carrying complex statistical weights $w(\omega) = \{w_{\Re}(\omega), w_{\Im}(\omega)\}$, where the signs of the real and imaginary parts of particle weights can be positive or negative. In [6], the complex cross section $\Sigma_0 + i\omega/v$ on the left-hand-side of Eq. (1) is dealt with explicitly by modifying the particle weights during flights. For our algorithm, we choose instead to work with a real cross section and we modify the collision kernel accordingly. This is achieved by following the strategy discussed in [10]: we add a term $\eta\omega/v\delta\Psi$, η being a real constant having the same sign as ω, to both sides of Eq. (1), and we move the term $i\omega/v\delta\Psi$ to the right-hand-side. Then, the equation becomes:

$$\left(\mathbf{\Omega}\cdot\nabla + \Sigma_0(\mathbf{r},E) + \eta\frac{\omega}{v}\right)\delta\Psi(\mathbf{r},\mathbf{\Omega},E,\omega) = \frac{\eta - i}{\eta}\eta\frac{\omega}{v}\delta\Psi(\mathbf{r},\mathbf{\Omega},E,\omega) + (...). \quad (4)$$

In this case, we work with a real modified total cross-section $\tilde{\Sigma}_0(\mathbf{r},E,\omega) = \Sigma_0(\mathbf{r},E) + \Sigma_\omega(E) > 0$ where $\Sigma_\omega(E) = \eta\omega/v > 0$. Hence, flight lengths are sampled as in standard Monte Carlo calculations, provided that $\tilde{\Sigma}_0$ is used instead of Σ_0.

Because of the structure of Eq. (4), the collision operator is now different from that of the regular Boltzmann equation, and we have to treat two types of particle productions: regular fission with probability $\Sigma_{0,f}/\tilde{\Sigma}_0$, and a special ω-production associated to a copy operator with probability $\Sigma_\omega/\tilde{\Sigma}_0$. We treat the regular fission as customary, i.e., the number of prompt or delayed fission neutrons is determined as $\mathrm{Int}(\nu_q\Sigma_{0,f}/\tilde{\Sigma}_0 + \xi)$ where Int(.) denotes the integer part, ξ is a uniform random number, and $q = p, d$. Because of the factor $\nu^j_{d,\omega}$ appearing in the delayed fission production term, the weight w_d of each new delayed neutron created by fission is modified to:

$$w_d = \frac{w}{k}\left(\frac{\lambda_j^2 - i\lambda_j\omega}{\lambda_j^2 + \omega^2}\right), \quad (5)$$

where w is the particle weight before the fission event. The term representing the ω-fission production consists of a copy of the incident neutron with a new weight w_ω given by:

$$w_\omega = w\frac{\eta - i}{\eta}. \quad (6)$$

Implicit capture (with forced fission) and Russian roulette can be used as in standard Monte Carlo method. Similarly as in [6], Russian roulette is applied separately to the absolute value of the real and imaginary parts of the particle weight: the particle is killed only if the real and the imaginary parts are both killed.

As described in [8], at low and very high frequencies, i.e., far from the plateau region of the zero-power reactor transfer function of the system (typically below 0.01 Hz and above 1 kHz), Monte Carlo methods for noise propagation lead to the production of a very large number of particles and the calculation time explodes. To perform simulations at low and very high frequencies, in [6] a weight cancellation technique is applied; the method proposed [8] does not need any weight cancellation technique and turns out to be rather robust. For the frequency region of interest for most applications in reactor noise analysis, i.e., approximatively between 0.01 Hz and 100 Hz, the algorithm described above converges safely with $\eta = 1$. Extreme cases beyond this frequency region have been also tested and calculations converge by suppressing implicit capture (and possibly tuning the η value as well at very high frequencies).

To summarize, our method (i) uses the conventional algorithm for fixed-source problems for all frequencies, (ii) does not need any weight cancellation technique, and (iii) is based on a real total cross-section and a modified collision kernel. The major advantage of this algorithm is that it introduces minimal modifications to standard Monte Carlo algorithms for particle transport (the key modification concerning the weight modification at delayed fission events and the special "copy" event) and can thus be implemented in continuous-energy production Monte Carlo codes such as TRIPOLI-4®. Scores such as flux and reaction rates over volumes and meshes have been extended in order to decompose the complex Monte Carlo estimators into modulus and phase, or equivalently real and imaginary part.

2.2.1. The noise source sampling method

In the general case, the noise source S is a complex function depending on the stationary flux Ψ_0 and the sign of its real and imaginary part can thus be space and/or energy-dependent. In order to sample arbitrary noise sources by Monte Carlo methods, we implemented in TRIPOLI-4® the following method: a standard power iteration is first run in order to determine Ψ_0 exactly. Convergence is achieved after a sufficient number of inactive cycles; then, each term in Eq. (3) is sampled by weighting the 'noise particles' generated by each component of S by the stationary collision density associated to Ψ_0. For instance, for the prompt fission term we would have

$$\frac{1}{k}\frac{\chi_p(E)}{4\pi}\iint \nu_p(E')\frac{\delta\Sigma_f(\mathbf{r},E',\omega)}{\Sigma_{0,f}(\mathbf{r},E')}\Sigma_{0,f}(\mathbf{r},E')\Psi_0(\mathbf{r},\mathbf{\Omega}',E')dE'd\mathbf{\Omega}', \tag{7}$$

which means that at fission events we would instantiate ν_p/k 'noise particles' with spectrum $\chi_p(E)$ and with a statistical weight $\delta\Sigma_f(\mathbf{r},E',\omega)/\Sigma_{0,f}(\mathbf{r},E')$ depending on the specific perturbation. By analogy with the strategy discussed in [11], a complete power iteration is performed once in the first batch: during the final cycle noise source particles are sampled so that the noise simulation can begin, while the generated fission neutrons are transferred to the second batch. This latter runs a few additional inactive cycles in order to ensure reasonable decorrelation between cycles before sampling the noise source for the second replica. The third batch gets the fission neutrons generated by the second one, and so on. In a parallel run, each processor would apply this strategy.

The proposed simulation scheme is illustrated in Fig. 1. The critical eigenvalue k that is required for the noise equations can be estimated during the first critical calculation, or be obtained from a separate calculation.

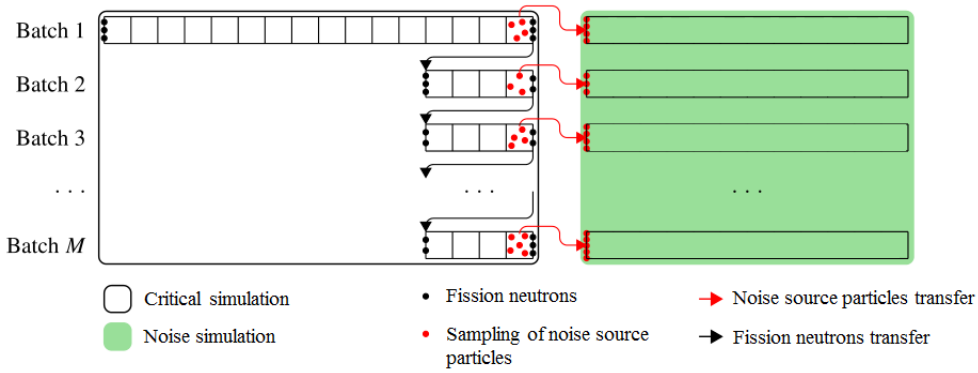

Figure 1: Neutron noise TRIPOLI-4® simulation process with M batches.

3. NUMERICAL VERIFICATIONS OF TRIPOLI-4® NEUTRON NOISE SOLVER

In this section, we briefly discuss some numerical verifications of the TRIPOLI-4® neutron noise solver against analytical solutions for an infinite homogeneous medium in the case of single-speed and continuous-energy problems, for an infinitely homogeneous cylindrical core, and for one-dimensional homogeneous core surrounded by a reflector. All Monte Carlo results (track length estimator) are plotted with their 1-σ error bars (barely visible in the figures).

3.1. Infinite homogeneous medium

For an infinite homogeneous medium in the case of single-speed problem, the results of the TRIPOLI-4® neutron noise solver are verified against analytical results (see [6] for the problem description and the analytical solutions). Here, the noise source is defined by $S = -1 + i$ at each frequency. Results are shown in Fig. 2: an excellent agreement is found.

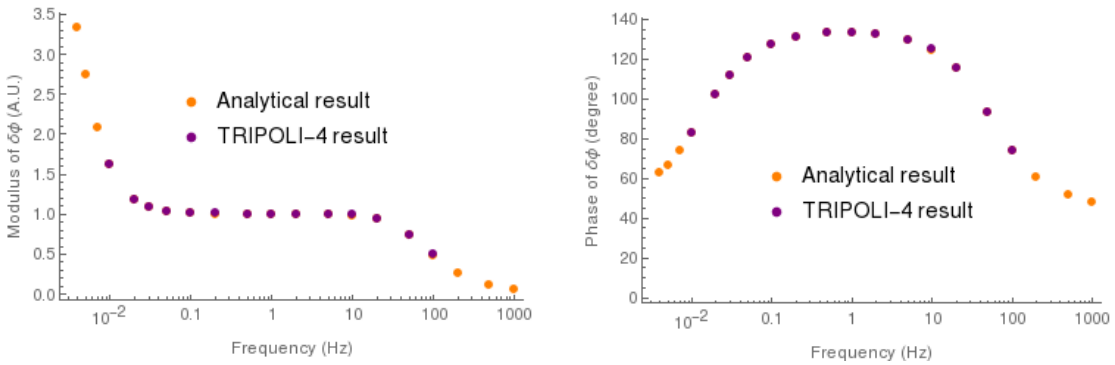

(a) Modulus of the neutron noise.

(b) Phase of the neutron noise.

Figure 2: Modulus and phase of $\delta\Psi(\omega)$ versus frequency in an infinite homogeneous medium (single-speed case).

For an infinite homogeneous medium in the case of continuous-energy problem, the result of our neutron noise solver is again verified against analytical results (see Fig. 3). Here, the noise source is defined by $S = 2 - 3i$ between 1 and 2 MeV and $S = -0.75 + 5i$ between 0.0001 and 0.0005 MeV at 3 Hz. For the sake of simplicity, for our tests we have modelled scattering by using a Maxwell spectrum and fission by a Watt spectrum. This example illustrates the capability of the neutron noise solver to correctly simulate continuous-energy problems.

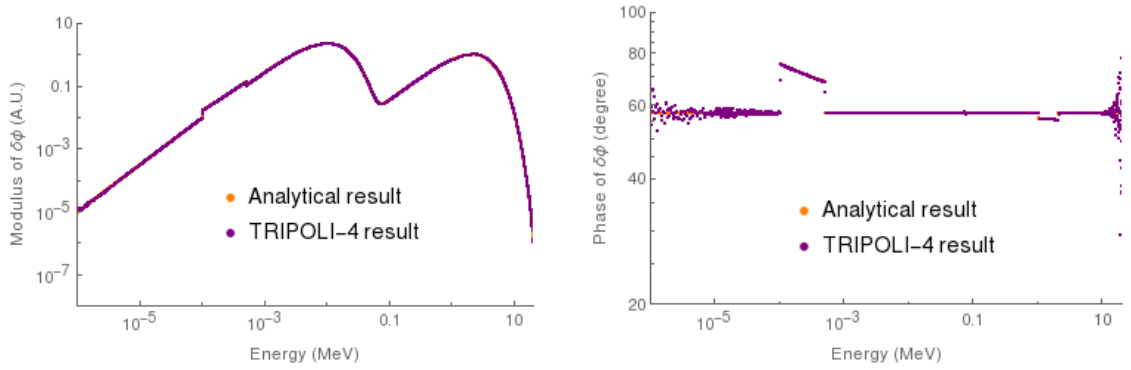

(a) Modulus of the neutron noise. (b) Phase of the neutron noise.

Figure 3: Modulus and phase of $\delta\Psi(\omega)$ versus energy at 3 Hz in an infinite homogeneous medium (continuous-energy case).

3.2. Infinitely-long homogeneous cylindrical core

We have further probed the noise solver in the case of an infinitely homogeneous cylindrical core with two energy groups (see [6] for all details of the problem data and analytical results in diffusion theory). Here, the noise source is defined by $S = -1$ for the thermal group at 1 Hz and at the center of the core. Results are shown in Fig. 4: some differences are observed at the center of the core, due to the expected slight discrepancies between solutions derived in diffusion theory and our transport results. Overall, the agreement is very satisfactory.

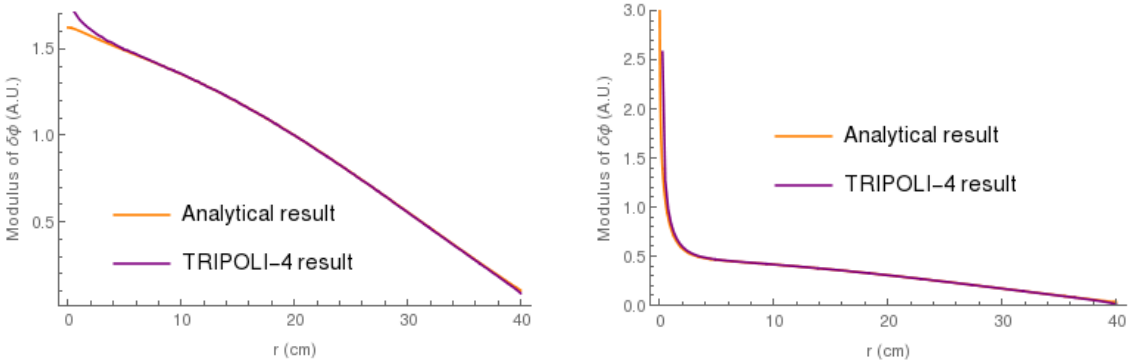

(a) Modulus of the fast neutron noise. (b) Modulus of the thermal neutron noise.

Figure 4: Modulus of $\delta\Psi(\omega)$ versus the radial position from the core center at 1 Hz in an infinitely-long homogeneous cylindrical core.

3.3. One-dimensional homogeneous core surrounded by a reflector

The final verification test concerns a one-dimensional homogeneous core surrounded by a reflector with two energy groups (see [4] for all details of the problem data and analytical results). Results are shown in Fig. 5. Here, the noise source is defined by $S = -3 - 0.5i$ for the fast group and $S = -1.2 + 2i$ for the thermal group at 1Hz and at the core/reflector interface. Again, an excellent agreement is found with respect to exact results.

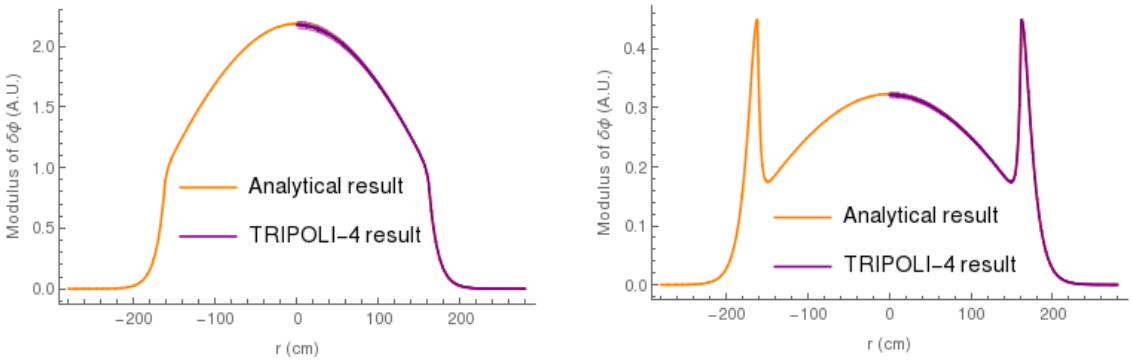

(a) Modulus of the fast neutron noise.

(b) Modulus of the thermal neutron noise.

Figure 5: Modulus of $\delta\Psi(\omega)$ versus position at 1 Hz in an one-dimensional homogeneous core surrounded by a reflector.

4. ANALYSIS OF NEUTRON NOISE IN A UOX PWR ASSEMBLY

We conclude our analysis by illustrating the capabilities of the TRIPOLI-4® neutron noise solver on a more realistic configuration, a standard UOX fuel assembly (see Fig. 6). We will first compare the induced neutron noise to the standard zero-power transfer function for the case of a simple delta-like noise source; then, we will consider the case of a vibration-induced noise source.

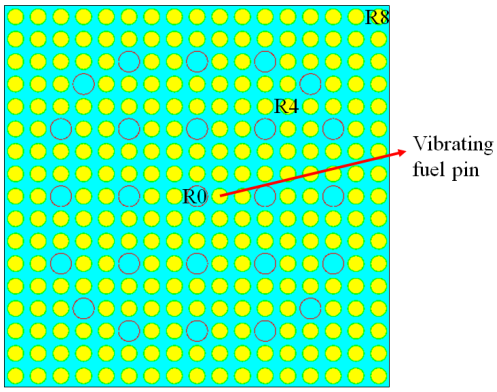

Figure 6: Top view of the UOX assembly.

4.1. An example of a simple noise source

We impose a simple isotropic noise source S at position $\mathbf{r}_0$ within the fuel assembly and energy E_0, with a given frequency ω_0. We compare the induced neutron noise $\delta\Psi(\omega)$ integrated over the

whole assembly to the zero-power transfer function $G_0(\omega) = 1/\left(i\omega\left(\Lambda_{\text{eff}} + \frac{\beta_{\text{eff}}}{i\omega+\lambda_{\text{eff}}}\right)\right)$, corresponding to the limit case of point-kinetics, i.e., a system responding to the perturbation insensitive of the space or energy effects. The position $\mathbf{r}_0$ of the noise source varies from the center to the top right corner of the system, occupying the center of the fuel rods (positions R0, R4 and R8 in Fig. 6). We tested different values for the energy E_0 of the noise source, i.e. 1 MeV, 1 KeV and 0.025 eV. Here for the sake of conciseness we show the results for $E_0 = 1$ keV. The angular frequency ω_0 takes values that are located in the 'plateau' region of G_0: physical perturbations in experimental and commercial reactors generally take place approximatively between $\omega_{low} = \lambda_{\text{eff}} \approx 0.1$ Hz and $\omega_{high} = \lambda_{\text{eff}} + \beta_{\text{eff}}/\Lambda_{\text{eff}} \approx$ a few tens of Hz.

In Fig. 7, we show the comparison between the modulus and the phase of $\delta\Psi(\omega)$ and G_0 as a function of the noise source position (R0, R4 and R8, see Fig. 6) at $E_0 = 1$ keV. As expected, we note that the computed neutron noise $\delta\Psi(\omega)$ slightly deviates from the point kinetics behaviour. As an illustration, Fig. 8 presents the spatially-resolved modulus and phase of $\delta\Psi(\omega)$ for the case of a noise source at position R4, energy 1 keV and frequency 30 Hz.

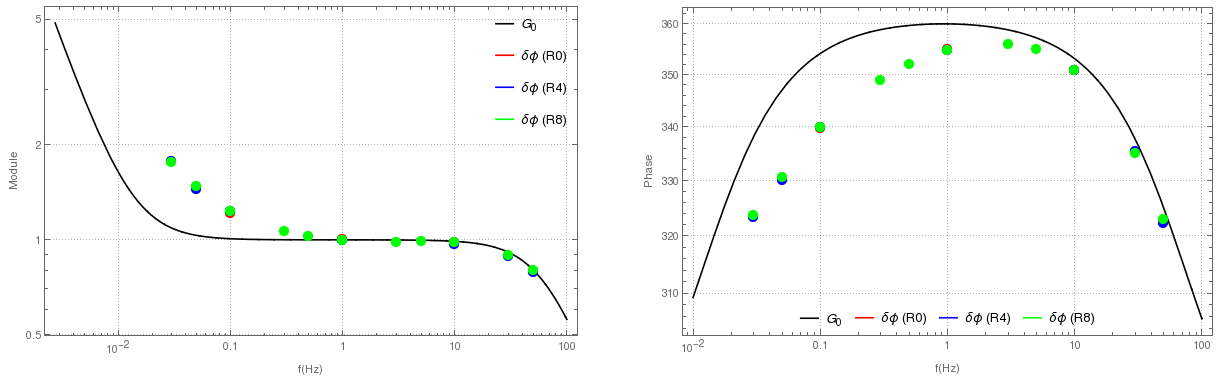

(a) Modulus of neutron noise (A.U.). (b) Phase of neutron noise (degrees).

Figure 7: Comparison between G_0 and $\delta\Psi(\omega)$ (modulus and phase) at 1 keV versus noise source position (R0, R4 and R8).

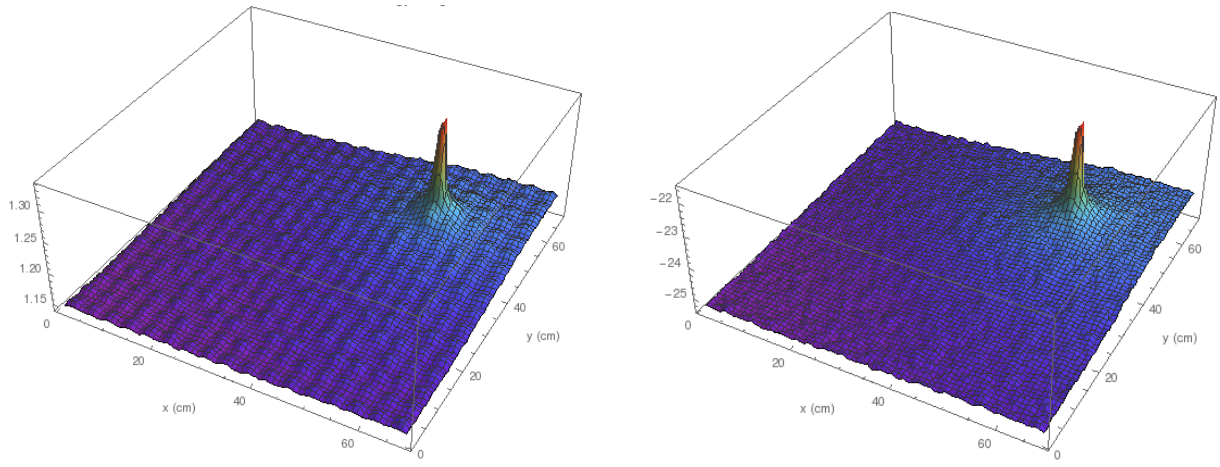

(a) Modulus of neutron noise (A.U.). (b) Phase of neutron noise (degrees).

Figure 8: Modulus and phase of $\delta\Psi(\omega)$ induced by a simple isotropic noise source at position R4, energy 1 keV and frequency 30 Hz.

4.2. An example of a vibration-induced noise source

We consider next the spatially-resolved modulus and phase of $\delta\Psi(\omega)$ induced by a fuel pin vibration along x-axis at 1 Hz with an amplitude of 0.1 cm (the position of the perturbed fuel pin is detailed in Fig. 6). The sinusoidal vibration model has been described in [12]. Results are shown in Fig. 9 for a noise source corresponding to a critical state Ψ_0 computed as detailed above.

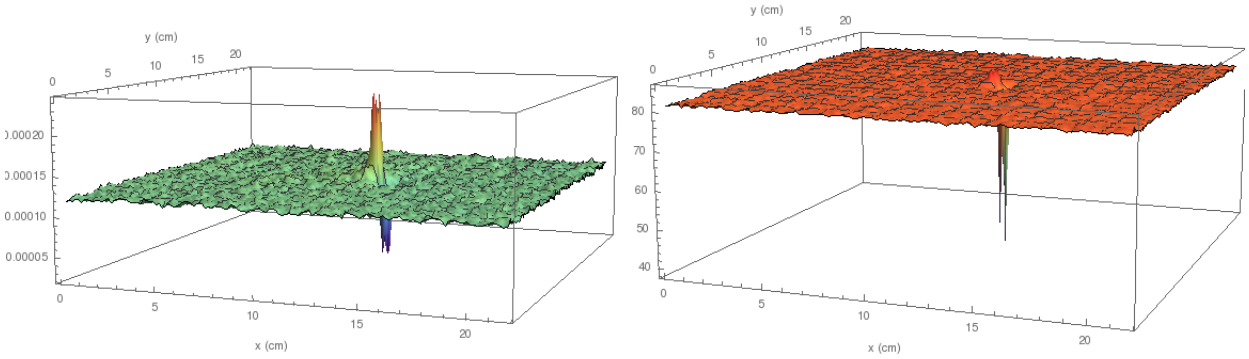

(a) Modulus of neutron noise (A.U.). (b) Phase of neutron noise (degrees).

Figure 9: Modulus and phase of $\delta\Psi(\omega)$ induced by a fuel pin vibration along x-axis at 1 Hz with an amplitude of 0.1 cm.

5. CONCLUSIONS

In this paper, we have presented the new TRIPOLI-4® solver for the neutron noise analysis in the frequency domain. Future work will concern the comparison with neutron noise simulations in the time and frequency domain performed with APOLLO3®, the multi-purpose deterministic transport code under development at CEA [13,14], and the validation of the developed solvers based on the new experimental campaigns carried out in the framework of the COLIBRI experimental program at the Crocus reactor (operated by EPFL, Lausanne, Switzerland) [15].

ACKNOWLEDGEMENTS

TRIPOLI-4® is a registered trademark of CEA. The authors thank Électricité de France (EDF) for partial financial support. The research leading to these results has received funding from the Euratom research and training programme 2014-2018 under grant agreement No 754316 (CORTEX project [16]).

REFERENCES

[1] Pázsit, I., Demazière, C., 2010. "Noise Techniques in Nuclear Systems". Handbook of Nuclear Engineering, Ed. D. G. Cacuci,3, 2, Springer Verlag.

[2] Fry, D. N. et al., 1986. "Use of Neutron Noise of Diagnosis of In-vessel Anomalies in Light-Water Reactors". ORNL/TM-8774.

[3] Jonsson, A. et al., 2012. "Analytical inverstigation of the properties of the neutron noise induced by vibrationg absorber and fuel rods". Kerntechnik 77, 371-380.

[4] Demazière, C., 2011. "CORE SIM: A multi-purpose neutronic tool for research and education". Annals of Nuclear Energy 38, 2698-2718.

[5] Malmir, H. et al., 2010. "Development of a 2-D 2-group neutron noise simulator for hexagonal geometries". Annals of Nuclear Energy 37, 1089-1100.

[6] Yamamoto, T., 2013. "Monte Carlo method with complex-valued weights for frequency domain analyses of neutron noise". Annals of Nuclear Energy 58, 72-79.

[7] Yamamoto, T., 2018. "Implementation of a frequency-domain neutron noise analysis method in a production-level continuous energy Monte Carlo code: Verification and application in a BWR". Annals of Nuclear Energy 115, 494501.

[8] Rouchon, A. et al., 2017. "A new Monte Carlo method for neutron noise calculations in the frequency domain". Annals of Nuclear Energy 102, 465-475.

[9] Brun, E. et al., 2015. "TRIPOLI-4®, CEA, EDF and AREVA reference Monte Carlo code". Annals of Nuclear Energy 82, 151-160.

[10] Zoia, A. et al., 2015. "Monte Carlo methods for reactor period calculations". Annals of Nuclear Energy 75, 627-634.

[11] Faucher, M. et al., 2018. "New kinetic simulation capabilities for TRIPOLI-4®: Methods and applications". Annals of Nuclear Energy 120, 74-88.

[12] Rouchon, A., Sanchez, R., 2015. "Analysis of Vibration-induced Neutron Noise using One-dimension Noise Diffusion Theory". International Congress on Advances in Nuclear Plants: Nuclear Innovations for a Low-Carbon Future (ICAPP 2015), Nice, France, May, 3-6.

[13] Gammicchia, A. et al., 2019. "Neutron kinetics equations in APOLLO3® code for application to noise problems". International Conference on Mathematics & Computational Methods Applied to Nuclear Science & Engineering (M&C 2019), Portland, USA, August 25-29.

[14] Rouchon, A. et al., 2017. "The new 3-D multigroup diffusion neutron noise solver of APOLLO3® and a theoretical discussion of fission-modes noise". International Conference on Mathematics & Computational Methods Applied to Nuclear Science & Engineering (M&C 2017), Jeju, Korea, April 16-20.

[15] Rais, A. et al., 2019. "Towards the validation of neutron noise simulators: qualification of data acquisition systems". International Conference on Mathematics & Computational Methods Applied to Nuclear Science & Engineering (M&C 2019), Portland, USA, August 25-29.

[16] Demazière, C. et al., 2018. "Overview of the CORTEX project". Reactor Physics Paving The Way Towards Mode Efficient Systems (PHYSOR 2018), Cancun, Mexico, April 22-26.